The Sunnydale landslide, current understanding and research, Dawson (NTS 116B/3)

Jackson Bodtker* and Dan Shugar
Water, Sediment, Hazards, and Earth-surface Dynamics (waterSHED) Lab, Department of Geoscience, University of Calgary

Derek C. Cronmiller and Jeffrey D. Bond
Yukon Geological Survey

Bodtker, J., Cronmiller, D.C, Bond, J.D. and Shugar, D., 2023. The Sunnydale landslide, current understanding and research, Dawson (NTS 116B/3). *In:* Yukon Exploration and Geology 2022, K.E. MacFarlane (ed.), Yukon Geological Survey, p. 19–33.

Abstract

The Sunnydale landslide is a slow-moving rock-slope deformation on the western bank of the Yukon River directly across from Dawson, Yukon. While recent data suggest acceleration of the slide, which could pose a potential hazard to Dawson if the acceleration continues to the point of rapid failure, limited data precludes certainty on probability and timing of this occurrence. Field mapping allowed for documentation of road subsidence, expanding tension cracks, recent and ongoing rockfall and production of detailed geomorphological and surficial geology maps of the slide. Differencing from 2014, 2018, 2019, 2020 and 2022 aerial lidar data, and data from physical monitoring stations indicate current movement rates of up to 11 cm/yr across the slide area. Ongoing work including terrestrial lidar change analysis and installation of a near-real-time monitoring system in early 2023 will increase our understanding of current movement trends. Additionally, in-progress geologic dating of deformation features will further our understanding of the history and context of this feature on a geologic timescale.

* Jackson.Bodtker@ucalgary.ca

Introduction

The Sunnydale landslide is an approximately 100 000 m^2 progressively developing rock slope deformation within an approximately 180 000 m^2 larger deep-seated gravitational slope deformation (DSGSD) located on the western bank of the Yukon River, directly across from Dawson, Yukon (Fig. 1). Rock slope instabilities of this nature are characterized by slow deformation on hundred-to-thousand-year timescales (Pánek and Klimeš, 2016; Hungr et *al.*, 2014). While many of these features pose little hazard and may never accelerate to the point of rapid failure, some do evolve into large destructive rock avalanche events (Pánek and Klimeš, 2016; Hungr et *al.*, 2014).

Forcing mechanisms that cause DSGSDs to progress into rapid rock avalanches can range from seismic activity to anomalously heavy rainfall or snowmelt that change porewater pressure in the slope (Pánek and Klimeš, 2016). Hilger et *al.* (2021) provide evidence for permafrost degradation as a trigger for reactivation and acceleration of DSGSDs while Chigira et *al.*, (2013) show that location above incising rivers can be a precursory influence. While these factors may both apply to the Sunnydale slide, no evidence of permafrost was found during fieldwork and ongoing influence of the river is likely small due to the location of the suspected failure plane approximately 30 m above water levels.

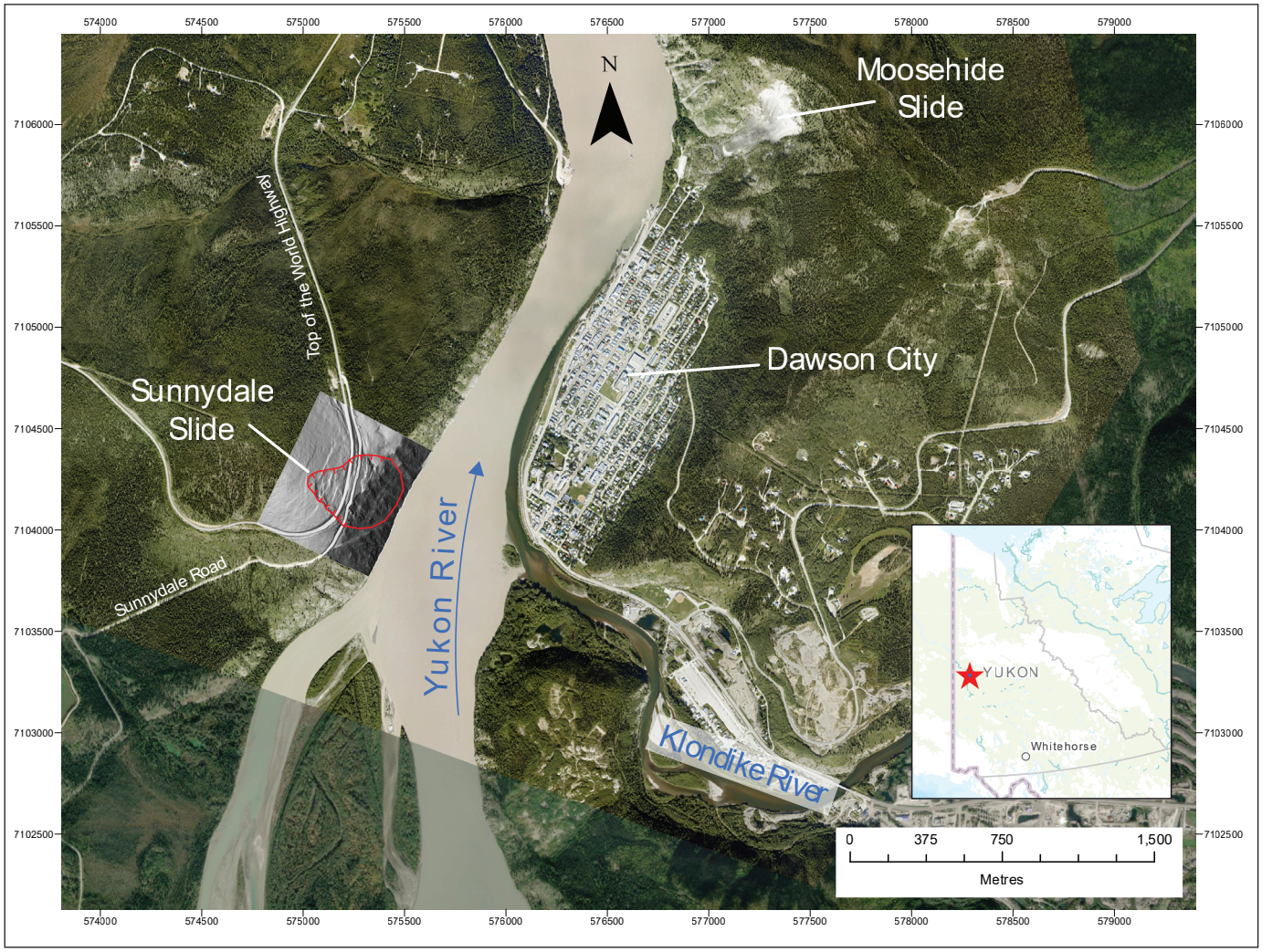

Figure 1. *Overview map showing the location of the Sunnydale slide relative to Dawson and the Klondike Valley. Satellite imagery from 2017 and 2020 (Esri, 2022) paired with lidar hillshade from 2022.*

The timing of the initial displacement is currently unknown; however, weathering on the upper portion of the headscarp suggests exposure for several thousand if not tens-of-thousands of years. Ages this old or older are possibly due to the slide location within Beringia, an area of Yukon that was not glaciated in the Quaternary (Duk-Rodkin, 1996; Froese *et al.*, 2000).

The landslide was first brought to the attention of the Yukon Geological Survey in 2020 by Dawson local Greg Hakonson; he made a connection between deformation along the Top of the World Highway and shallow landslide activity on the steeper front above the Yukon River (Pers. Comm.). Peter Nagano, road foreperson for the Dawson region, stated that the deformation of the Top of the World Highway road surface has been noticeable for approximately 30 years but has gotten worse in the last six years (Pers. Comm.). Further investigation by the Yukon Geological Survey confirmed the presence of the landslide and concerns were such that engineering firm BGC was hired to perform a preliminary investigation (BGC 2020a). This report included an initial map of the area, initial lidar-based change detection, and a recommendation for further study. A second report from BGC estimated the annual failure probability to be between 0.0005 and 0.009 or an approximately 15% chance in the next 50 years (BGC, 2020b).

Regional setting

Bedrock in the slide area is mapped as the Dawson–Clinton Creek unit, a part of the Yukon-Tanana terrane. The unit consists of metavolcanic and metasedimentary rocks including greenstone, phyllite and metachert of Permian age. While no faults are mapped across the slide itself, the local area is cut by several thrust faults (Mortensen, 1988).

The Yukon River has played an extensive role in shaping the Dawson region throughout the Quaternary. Until the latest Pliocene, the Yukon River flowed to the south with headwaters north of Dawson. Following the formation of Glacial Lake Yukon, and contemporaneous with its drainage, the river reversed drainage at about 2.64 Ma (Tempelman-Kluit 1980; Froese *et al.*, 2000; Hidy *et al.*, 2012). This reversal greatly expanded the drainage area of the river and began down-cutting, which formed the slope on which the Sunnydale slide is located. Loess sedimentation has occurred during glacial periods throughout the Quaternary (Fraser and Burn, 1997).

The Dawson area contains numerous other rockslides. The Moosehide slide, for example, has been a key landmark of the region since time immemorial and several other prehistoric rockslide deposits have been mapped throughout the region (McKenna and Lipovsky, 2014). The Moosehide slide has been studied in detail (Brideau *et al.*, 2007, 2012; BGC, 2020b, 2021a,b) and recently instrumented with a near-real-time monitoring system consisting of GNSS-Rovers, extensometers, tiltmeters and a weather station (BGC, 2021c).

Climate records dating to 1901 show an average annual air temperature of -4.58°C and average annual precipitation of 323.37 mm (Environment Canada, 2022). Dawson and the Sunnydale landslide are located within the zone of extensive discontinuous permafrost (Heginbottom *et al.*, 1995). While a detailed regional model suggests a 0.7 to 0.8 probability of permafrost on the slope (Bonnaventure *et al.*, 2012), no evidence of permafrost was observed during field investigations or desktop analysis.

The Dawson region experiences only minor seismic activity. Small, infrequent, local earthquakes under magnitude four have been observed in the Dawson area over the last century. Larger events occur more regularly to the north and south of the region but at distances from the Sunnydale landslide that make them unlikely to act as a landslide trigger (*cf.,* Keefer, 1984).

Geomorphological mapping and geologic history

A combination of airborne lidar, aerial photos and field mapping was used to identify and characterize geomorphic features and variations in surficial and bedrock geology (Figs. 2 and 3). The landslide consists of two main geomorphic areas. The lower half of the slide (roughly 50 000 m^2) is a steep, sparsely vegetated face consisting of bedrock, boulder fields, and mixed loess and bedrock colluvium. The upper half (roughly 50 000 m^2) is characterized by gentler slopes, spruce forests and a covering of loess and mixed loess and weathered bedrock colluvium. The headscarp is approximately 6 m in height and 150 m long, and displays three distinct degrees of weathering and vegetation cover that increase with height (Fig. 4). Competent bedrock is best exposed at the southern margin of the slide at TCMS station 3 (Fig. 2). The headscarp here has a strike and dip of 300/75 and slickenlines covering the bottom ~1 m at a plunge and trend of 67/070 (Fig. 4). The bedrock forming the headscarp becomes increasingly, but non-linearly, weathered and vegetated first with lichen and then moss and grasses towards the top. These differences may indicate episodic movement on a timescale of thousands to tens of thousands of years. Rock samples taken from the headscarp are being analyzed for cosmogenic-nuclide measurement to determine the timing of surface exposure and to further elucidate a chronology of prehistoric movement.

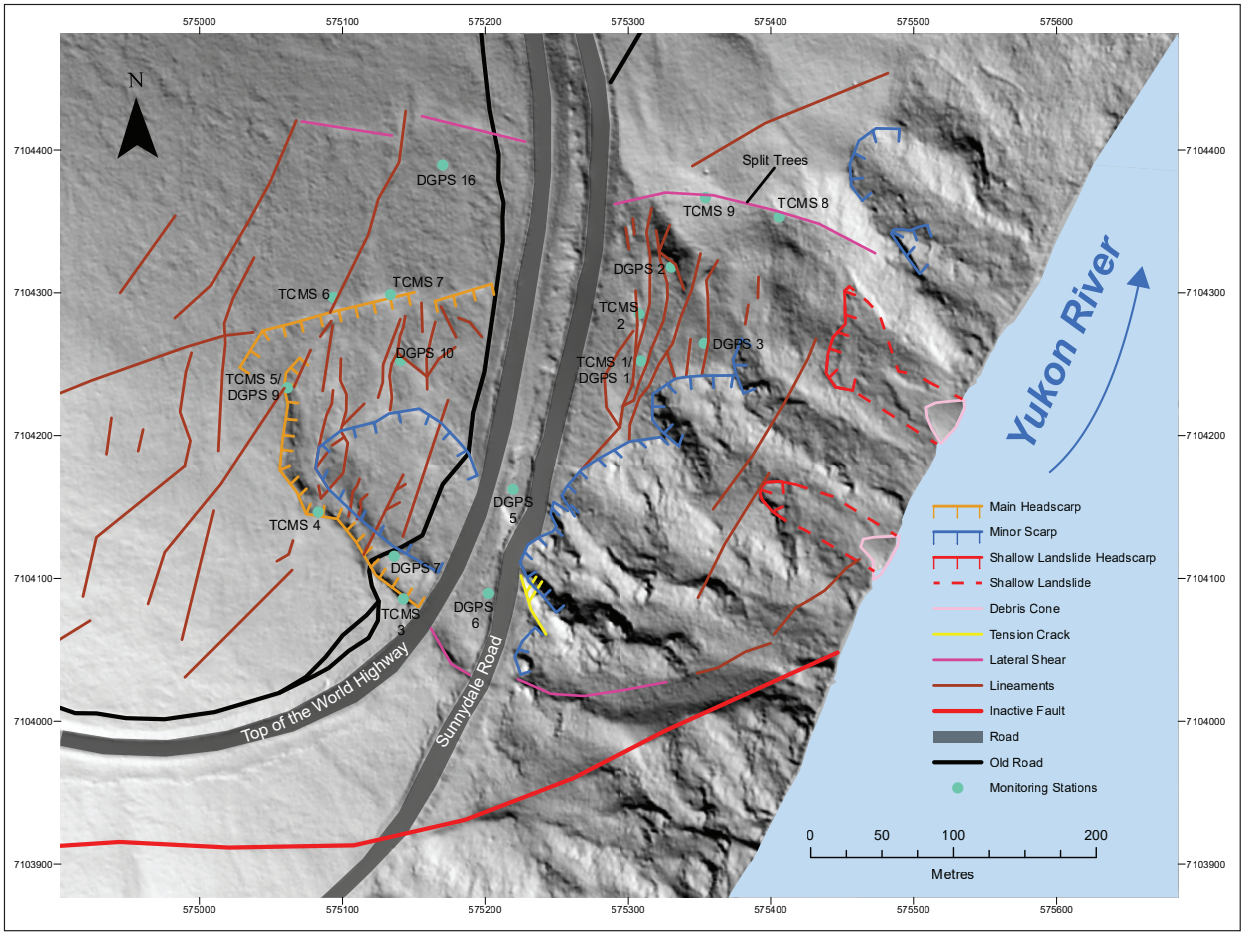

Figure 2. *Geomorphological map of the Sunnydale slide including locations of DGPS and TCMS physical monitoring stations.*

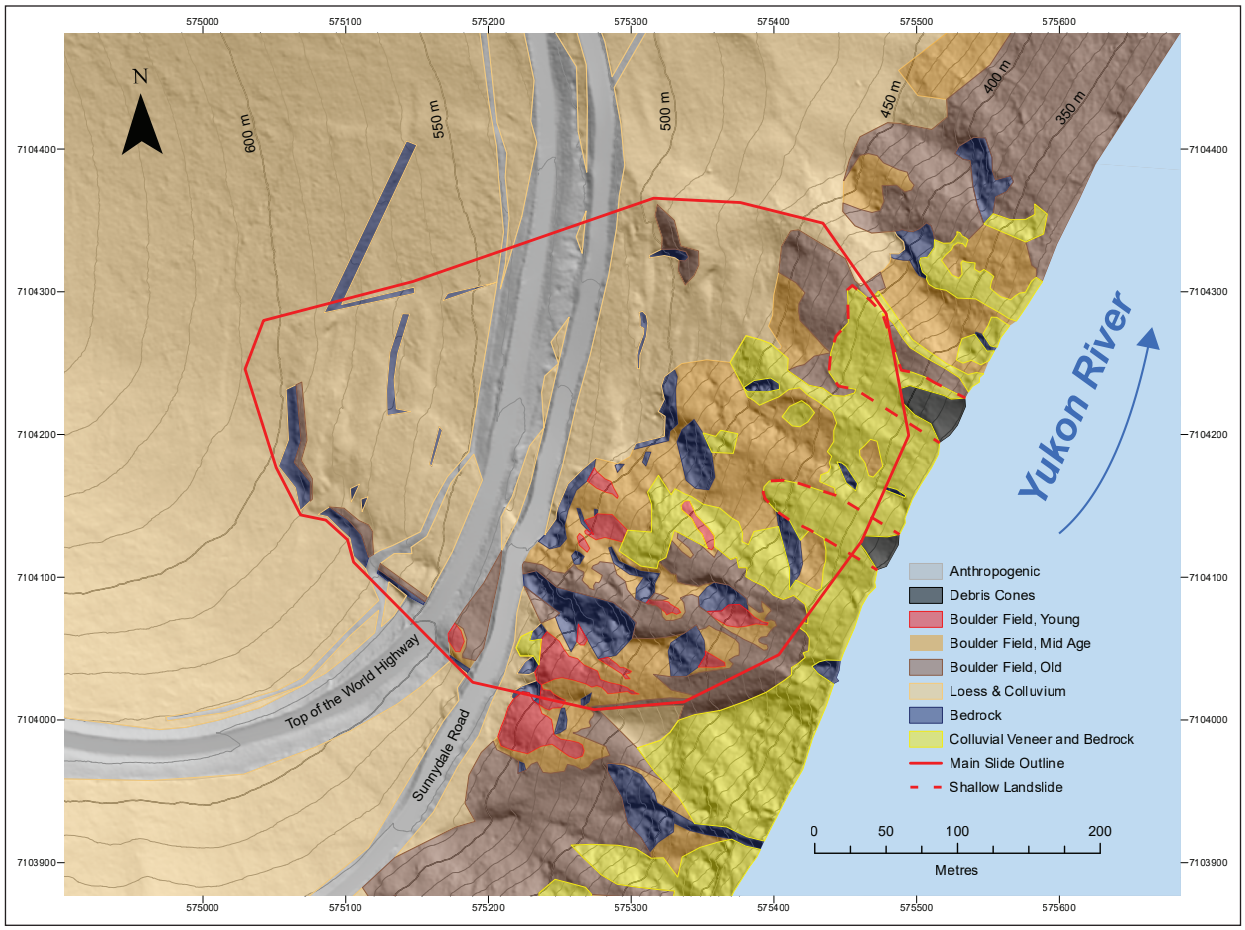

Figure 3. *Surficial geology map of the Sunnydale slide.*

Figure 4. (a) *The headscarp of the slide near TCMS station 3. Note the distinct change in vegetation at approximately waist height.* ***(b)*** *Slickenlines on the headscarp.*

Many of the lineaments mapped on the upper half of the slide consist of sediment-filled grabens or tension cracks. Several of these features were investigated using soil trenches to document the stratigraphy of the sediments that have filled them (Fig. 5). Tephra from the northern lobe of the White River ash volcanic event found within these features date them to approximately 1625 years old (Reuther *et al.*, 2020) providing a current minimum age of displacement; however this minimum age is expected to be a significant underestimate. Results from additional ongoing dating work will further constrain minimum age of opening of these features.

Two shallow landslides are present at the toe of the main slide; each is 1–3 m deep and has an approximate volume of 1000–3000 m^3. The northern landslide

Figure 5. (a) *Tension crack near TCMS station 2. Recent movement is shown by the gap between the rock and moss growth.* ***(b)*** *TCMS station 6.* ***(c)*** *Split tree near TCMS 8 with nail monitoring installed. This crack opened 2.2 cm and 3.3 cm between June and September 2022 at the upper and lower nail sets respectively.* ***(d)*** *Terrestrial lidar scanner with the Sunnydale slide in the background across the Yukon river, note the shallow landslide directly left of the scanner.*

initially failed in 2018, while the southern slide occurred in 2019. While both slides continue to grow, the northern slide has experienced significant enlargement as recently as September 2022. These slides are likely related to over-steepening at the toe of the larger Sunnydale rock mass as it pushes out towards the river (Fig. 6).

Extensive bedrock exposure across many areas of the slide allowed for analysis through use of joint and fabric mapping as well as Geological Strength Index (GSI) characterization. Prior work used these techniques for preliminary slope stability analysis and the new data will be added to enhance any future modeling work (BGC, 2021a). GSI results span a wide range of values from 5–75 with a mean of 43. These results indicate blocky, disturbed and disintegrated rock across the slide area (Hoek and Brown, 1997).

Current measurable motion is constrained to an area of approximately 100 000 m^2 but evidence of past deformation exists across much of the adjacent hillslope, encompassing an area of approximately 180 000 m^2. While the depth of the failure plane is uncertain, lidar differencing and geomorphic evidence have allowed for an approximate delineation of a daylighting surface on the face of the slide (Fig. 6).

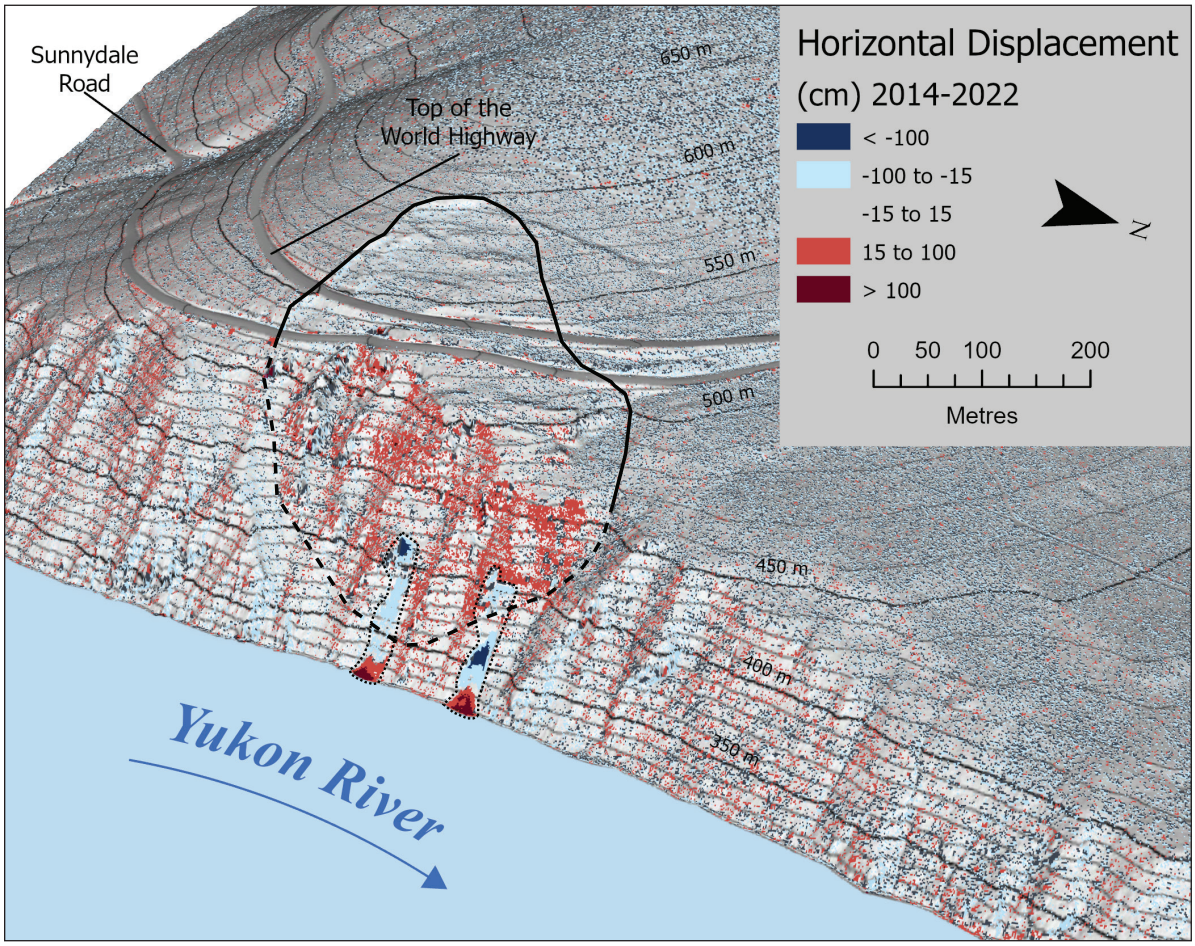

Figure 6. *Horizontal lidar differencing between 2014 and 2022 aerial lidar data. Dashed line indicates the inferred failure plane where it daylights on the steep river cut slope. Solid line shows the approximate upper extent of the slide. Two small shallow landslides are visible and indicated by dotted lines.*

Physical displacement monitoring

Three types of physical monitoring stations are currently in use on the landslide; GPS pin stations (DGPS; Table 1), tension crack monitoring stations (TCMS; Table 2), and nails in split trees (NT; Fig. 5; Table 2). The DGPS consist of a single rebar pin, these stations were installed on July 2 and 3, 2021 by Jeffrey Bond and Peter von Gaza. The TCMS consist of two rebar pins spanning a tension crack or scarp feature to assess rates of opening. TCMS 1 to 5 were established by Jeffrey Bond and Peter von Gaza coincidentally with the DGPS stations while TCMS 6 to 9 were established by Jackson Bodtker and Holly Basiuk on June 24 and 30, 2022. The NT stations consist of trees that have been split due to differential ground motion below them (Fig. 5), and were installed by Jackson Bodtker and Holly Basiuk on June 30, 2022.

Results from comparing repeat DGPS measurements show significant and potentially accelerating movement of 6 to 11 cm/year across the slide since installation (Figs. 7, 8 and 9; Table 1). TCMS measurements also indicate motion on the slide (Fig. 10).

Table 1. *Differential GPS station locations and change analysis.*

Station	Number	UTM Position (m)								
		2–3 July 2021			22 June 2022			7 October 2022		
		Easting	Northing	Height	Easting	Northing	Height	Easting	Northing	Height
DGPS	1	575308.319	7104267.632	510.257	575308.441	7104267.603	510.194	575308.485	7104267.612	510.181
	2	575330.931	7104315.234	499.335	575331.117	7104315.225	499.267	575331.164	7104315.224	499.215
	3	575355.352	7104283.389	485.159	575355.498	7104283.386	485.102	575355.536	7104283.376	485.05
	4	575283.442	7104361.339	514.886	Destroyed					
	5	575222.011	7104164.164	539.44	575222.102	7104164.145	539.404	575222.115	7104164.141	539.389
	6	575199.443	7104077.596	532.936	575199.524	7104077.601	532.868	575199.545	7104077.588	532.839
	7	575139.777	7104111.815	562.111	575139.835	7104111.805	562.053	575139.865	7104111.795	562.047
	9	575064.509	7104235.78	594.638	575064.558	7104235.774	594.641	No Measurement		
	10	575145.015	7104250.971	567.998	575145.094	7104250.971	567.929	575145.126	7104250.964	567.895
	16	Measurement Error			575162.638	7104385.318	555.95	575162.639	7104385.313	555.932

Station	Number	Change (cm)								
		July 2021 – June 2022			June 2022 – Oct. 2022			July 2021 – Oct. 2022		
		Easting	Northing	Height	Easting	Northing	Height	Easting	Northing	Height
DGPS	1	-12.2	2.9	-6.3	-4.4	-0.9	-1.3	-16.6	2.0	-7.6
	2	-18.6	0.9	-6.8	-4.7	0.1	-5.2	-23.3	1.0	-12.0
	3	-14.6	0.3	-5.7	-3.8	1.0	-5.2	-18.4	1.3	-10.9
	4	Destroyed								
	5	-9.1	1.9	-3.6	-1.3	0.4	-1.5	-10.4	2.3	-5.1
	6	-8.1	-0.5	-6.8	-2.1	1.3	-2.9	-10.2	0.8	-9.7
	7	-5.8	1.0	-5.8	-3.0	1.0	-0.6	-8.8	2.0	-6.4
	9	-4.9	0.6	+0.3	N/A			N/A		
	10	-7.9	0.0	-6.9	-3.2	0.7	-3.4	-11.1	0.7	-10.3
	16	N/A			-0.1	0.5	-1.8	N/A		

Table 2. *Tension crack and split tree monitoring station locations and change analysis.*

Station Type	Number	Measurements (cm)				Change (cm)		Error (cm)	Latitude	Longitude
		2–3 July 2021	23 May 2022	23–30 June 2022	22 Sept. 2022	July 2021 – Sept. 2022	June – Sept. 2022			
TCMS	1	660.5	661.0	661.3	661.0	0.5	-0.3	1.0	64.05691	-139.45706
	2	788.7	790.0	790.0	789.8	+1.0	-0.2		64.05714	-139.45718
	3 U	92.6	94.4	94.5	94.8	+2.2	+0.3		64.05531	-139.46050
	3 L	56.0	57.0	57.3	57.6	+1.6	+0.3			
	4	695.9	N/A	699.0	698.5	+2.6	-0.5		64.05583	-139.46160
	5	405.0		409.0	409.5	+4.5	+0.5		64.05667	-139.46220
	6	N/A		721.5	720.7	N/A	-0.8		64.05716	-139.46148
	7			713.0	713.3		+0.3		64.05725	-139.46049
	8			790.7	797.2		+6.5		64.05766	-139.45545
	9			708.5	709.5		+1.0		64.05782	-139.45608
Split Trees	1 Upper	N/A	N/A	13.2	12.8	N/A	-0.4	0.2	64.05782	-139.45662
	1 Lower			23.4	22.8		-0.6			
	1.5			7.2	7.0		-0.2			
	2 Upper			11.9	12.4		+0.5		64.05785	-139.45631
	2 Lower			23.5	24.3		+0.8			
	3 Upper			14.6	14.7		+0.1		64.05774	-139.45577
	3 Middle			33.2	33.4		+0.2			
	3 Lower			41.9	42.4		+0.5			
	4 Upper			23.5	25.7		+2.2		64.05766	-139.45545
	4 Lower			43.7	47.0		+3.3			

Displacements across TCMS 1 and 2 of less than 1 cm/year compared to 16.6 to 23.3 cm of eastward change seen at adjacent DPGS 1, 2 and 3 indicate that these tension cracks are not currently opening, and this area of the slide is likely moving as a larger semi-coherent block. TCMS 3, 4 and 5 are located along the margins of the slide and show 1 to 3 cm/year movement relative to areas with less or no current motion. TCMS 6 to 9 only have measurements across ~3 months from June to September 2022, yet TCMS 8 shows an alarming 6.5 cm of motion on the northern margin of the slide during this time. We assume up to 1 cm of error in these measurements due to approximately 0.5 cm of flex at each rebar pin.

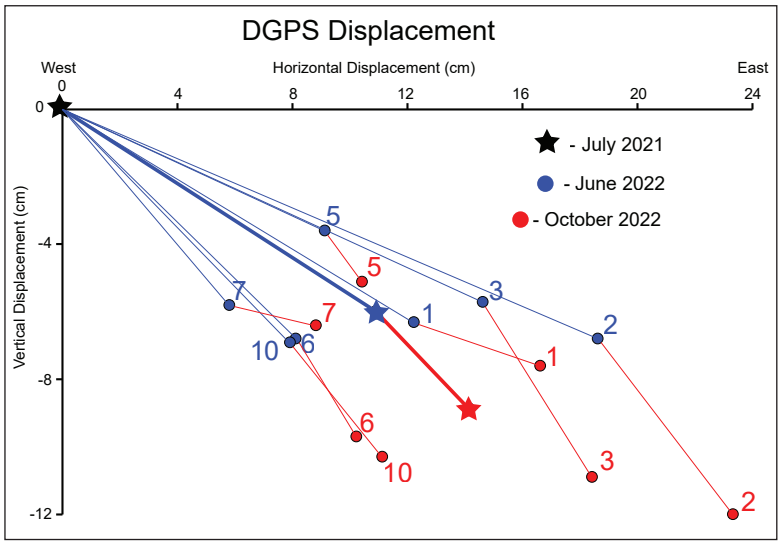

Figure 7. *Vertical and horizontal displacement observed at DGPS stations. Positions from the original July 2021 measurements have been normalized to the origin. Stars indicate average values given time intervals.*

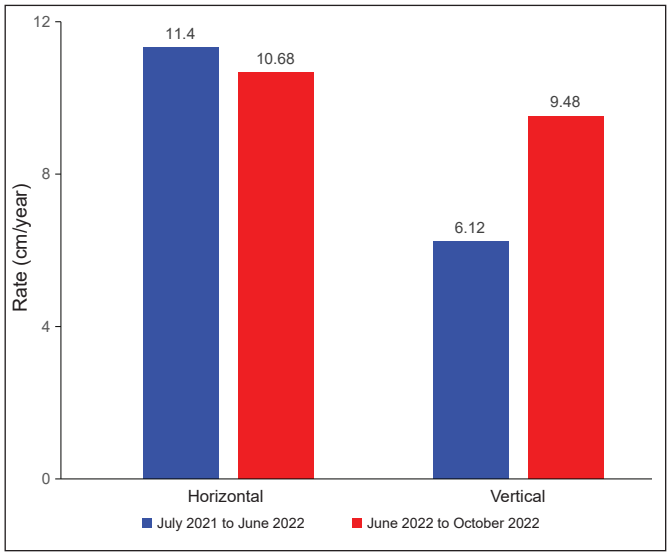

Figure 8. *Average rate of change in the vertical and horizontal directions observed at DGPS stations from July 2021 to June 2022 and June 2022 to October 2022.*

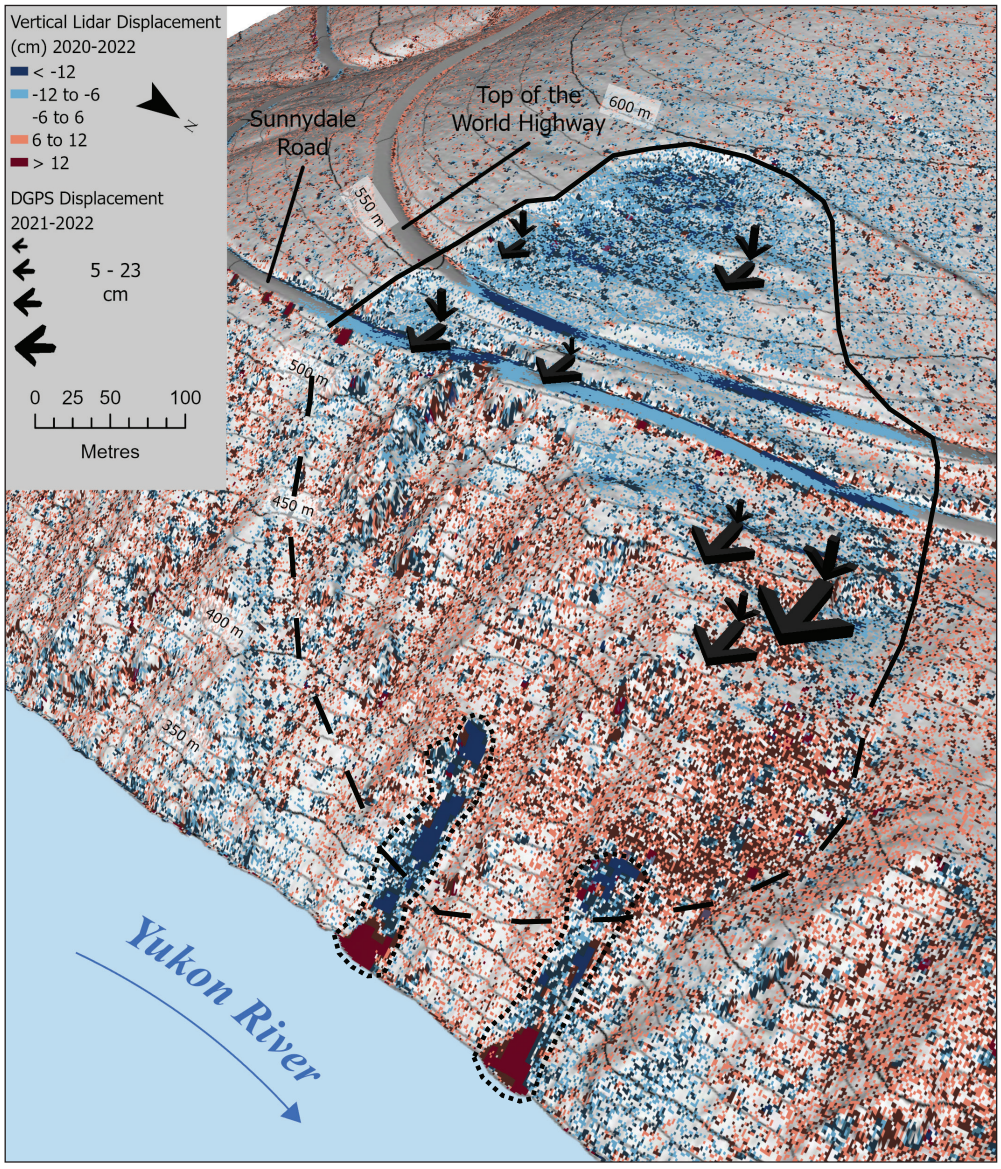

Figure 9. *Vertical lidar displacement from 2020 to 2022 overlain by arrows showing measured vertical and horizontal displacement at DGPS stations from 2021 to 2022 (see Fig. 7).*

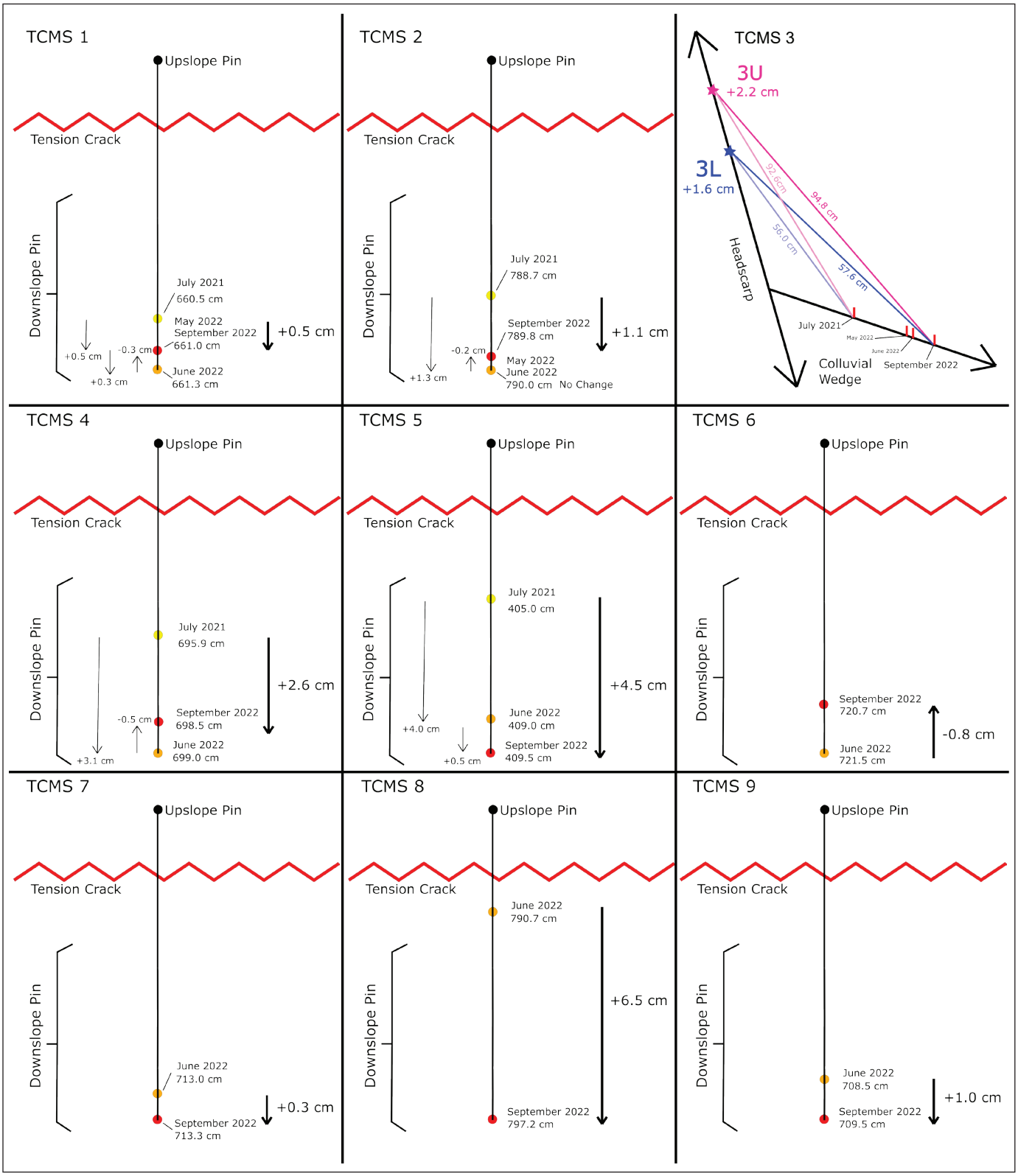

Figure 10. *Periodic measurement of displacement across tension cracks and scarps. See figure 2 for station locations.*

Lidar change analysis

Aerial lidar data from 2014, 2018, 2019, 2020 and 2022 were analyzed to characterize changes to the ground surface (Table 3). Point clouds were registered and analyzed using cloud to cloud distance differencing in CloudCompare (CloudCompare, 2022). Differencing was completed for 2014 to 2018, 2018 to 2019, 2019 to 2020, 2020 to 2022, 2014 to 2022, and 2018 to 2022. Deviations in positions of points between years were split into x, y and z components with the z-axis oriented vertically and the x-axis oriented at 110°, perpendicular to the Yukon River, and approximately parallel to the direction of horizontal ground motion observed from DGPS data. Rasters with a one-metre cell size were created from the final differenced point clouds (Figs. 6, 9 and 11)) and the surface of the Top of the World Highway was subsampled down to 500 randomly distributed points to compare change along the z-axis. The road surface was chosen due to the lack of noise associated with lidar pulse returns on vegetated surfaces and the relatively flat surface minimizing vertical error arising from small differences in nearest-point locations between collection years. Results from these data show continuing vertical drop (3–5 cm/year) throughout the period of available data (Fig. 12). Ongoing work will further analyze airborne lidar data and incorporate repeat terrestrial lidar scans completed during June and September of 2022.

Conclusions

Current rates of motion on the Sunnydale slide paired with its volume and location adjacent to the community of Dawson make this one of the highest priority geohazards in the Yukon. Work in progress to further understand this landslide includes implementation of a near-real-time GNSS monitoring system on the slide,

Table 3. *Lidar metadata and subsample change analysis.*

Station	Range	Change (cm)					Mean Rate (cm/year)
		Minimum	Maximum	Mean	Median	Standard Deviation	
Lidar Subsample	2014–2018	-32	13	-15	-15	4	3.64
	2018–2019	-8	12	-3	-3	2	2.96
	2019–2020	-12	10	-3	-3	3	3.34
	2020–2022	-16	13	-9	-9	3	4.93

	Date	Vertical Accuracy (m)	Point Density (ppm)	Source	Horizontal Datum	Vertical Datum	Projection
Lidar Data	Sept. 8 and 15, **2014**	0.119	7.5	Government of Yukon Lidar Repository (Contractor: McElhanney)	NAD83(CSRS)	CGVD28	UTM Zone 7N
	Sept. 19, 21 and 29, **2018**	0.14	10.7				
	June 7, 11 and 13, **2019**	0.02	18.4				
	Aug. 19, **2020**	0.05	18.1				
	June 17, **2022**	0.021	11.7				

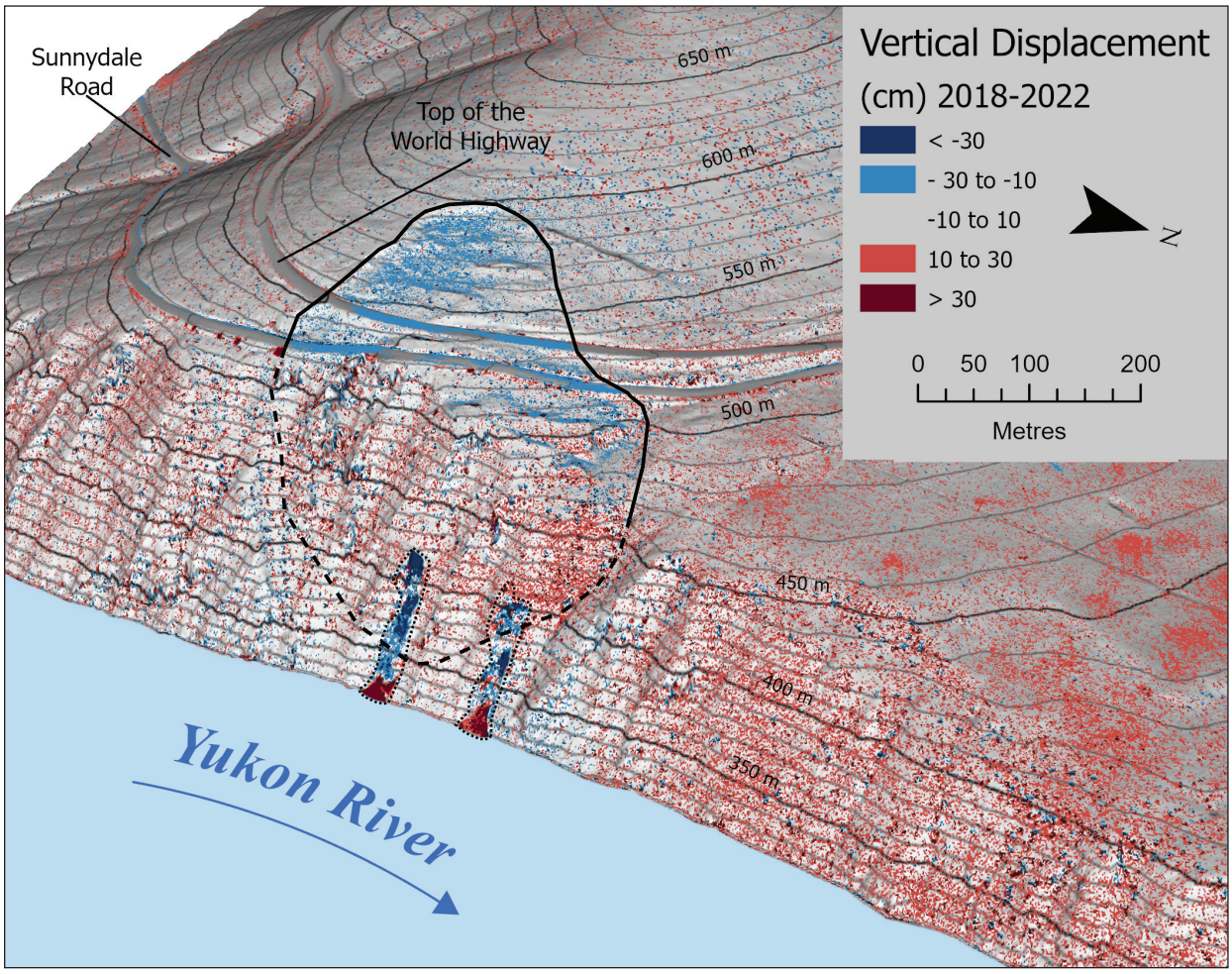

Figure 11. *Vertical displacement from aerial lidar differencing from 2018 to 2022. Anomalous areas of elevation gain north of the slide area are likely due to discrepancies in last return picking across different years.*

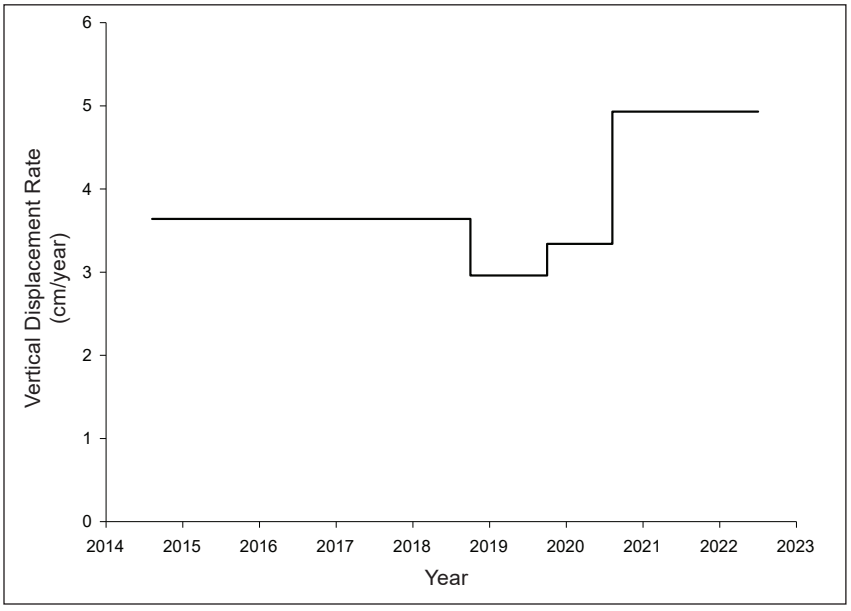

Figure 12. *Vertical displacement along the Top of the World highway from aerial lidar data. Values are the mean of 500 randomly-distributed points along the roadway within the boundaries of the main slide.*

repeat lidar surveys and a variety of dating analyses to further our understanding of the timing and rate of prehistoric movement. Additional complimentary work is being undertaken by several consultants to further constraint the current rates of movement and model theoretical rapid failure scenarios. This ongoing work will help us evaluate the risk posed to the community by the Sunnydale slide and set a standard for landslide assessment monitoring in the territory.

Acknowledgements

The authors would like to thank field assistant Holly Basiuk, as well as Dawson locals Peter Nagano and Greg Hakonson for sharing their knowledge of the slide. Funding from the Yukon Geological Survey, the Northern Scientific Training Program, the Geological Society of America and the Natural Sciences and Engineering Research Council of Canada (grant #DG-2020-04207) was invaluable to completion of this work. Dr. Gioachino Roberti is sincerely thanked for his helpful review. Finally, we would like to thank the Tr'ondëk Hwëch'in First Nation for granting us access to their lands and traditional territory.

References

BGC, 2020a. Initial Site Visit at Sunnydale Slide. Unpublished Report, 39 p.

BGC, 2020b. Initial Site Visit at the Moosehide Landslide. Unpublished Report, 23 p.

BGC, 2021a. Sunnydale Slide Deformation Mechanism and Preliminary Failure Probability. Unpublished Report, 23 p.

BGC, 2021b. Moosehide Landslide Hazard Characterization. Unpublished Report, 32 p.

BGC, 2021c. Moosehide Landslide – Dawson City, Yk, Quantitative Risk Assessment. Unpublished Report, 58 p.

Bonnaventure, P.P., Lewkowicz, A.G., Kremer, M. and Sawada, M., 2012. A regional permafrost probability model for the southern Yukon and northern British Columbia, Canada. Permafrost and Periglacial Processes, vol. 23, p. 52–68, https://doi.org/10.1002/ppp.1733.

Brideau, M.-A., Stead, D., Roots, C. and Lipovsky, P.S., 2012. Ongoing displacement monitoring at the Dawson City landslide (Dawson map area NTS 116B/3). In: Yukon Exploration and Geology 2011, K.E. MacFarlane and P.J. Sack, (eds.), Yukon Geological Survey, p. 17–26.

Brideau, M.-A., Stead, D., Stevens, V., Roots, C., Lipovsky, P. and Von Gaza, P., 2007. The Dawson City landslide (Dawson map area, NTS 116B/3), central Yukon. *In:* Yukon Exploration and Geology 2006, D.S. Emond, L.L. Lewis and L.H. Weston (eds.), Yukon Geological Survey, p. 123–137.

Chigira, M., Tsou, C.-Y., Matsushi, Y., Hiraishi, N. and Matsuzawa, M., 2013. Topographic precursors and geological structures of deep-seated catastrophic landslides caused by Typhoon Talas. Geomorphology, vol. 201, p. 479–493, https://doi.org/10.1016/j.geomorph.2013.07.020.

CloudCompare (version 2.12.4), 2022. GPL software. Retrieved from http://www.cloudcompare.org/.

Duk-Rodkin, A., 1996. Surficial geology, Dawson, Yukon Territory. Geological Survey of Canada, Open File 3288, scale 1:250 000, https://doi.org/10.4095/207910.

Environment Canada, 2022. National Climate Data and Information Archive, https://climate.weather.gc.ca/historical_data/search_historic_data_e.html, [accessed November 7, 2022].

Esri, 2022. World Imagery, https://www.arcgis.com/home/item.html?id=10df2279f9684e4a9f6a7f08febac2a9, [accessed December 6, 2022].

Fraser, T.A. and Burn, C.R., 1997. On the nature and origin of "muck" deposits in the Klondike area, Yukon Territory. Canadian Journal of Earth Sciences, vol. 34. p. 1333–1344, https://doi.org/10.1139/e17-106.

Froese, D.G., Barendregt, R.W., Enkin, R.J. and Baker, J., 2000. Paleomagnetic evidence for multiple Late Pliocene - Early Pleistocene glaciations in the Klondike area, Yukon Territory. Canadian Journal of Earth Sciences, vol. 37, p. 863–877.

Heginbottom, J.A., Dubreuil, M.A. and Harker, P.A., 1995. Canada – Permafrost. In: The National Atlas of Canada, 5th edition, Natural Resources Canada, MCR Series no. 4177, Plate 2.1: MCR4177.

Hidy, A.J., Gosse, J.C., Sanborn, P. and Froese, D.G., 2012. Age-erosion constraints on an Early Pleistocene paleosol in Yukon, Canada, with profiles of 10Be and 26Al: Evidence for a significant loess cover effect on cosmogenic nuclide production rates, Quaternary Science Reviews, vol. 165, p. 260–271.

Hilger, P., Hermanns, R.L., Czekirda, J., Myhra, K.S., Gosse, J.C. and Etzelmüller, B., 2021. Permafrost as a first order control on long-term rock-slope deformation in (Sub-)Arctic Norway. Quaternary Science Reviews, vol. 251, https://doi.org/10.1016/j.quascirev.2020.106718.

Hoek, E. and Brown, E.T., 1997. Practical estimates of rock mass strength. International Journal of Rock Mechanics and Mining Sciences, vol. 34, p. 1165–1186, https://doi.org/10.1016/S1365-1609(97)80069-X.

Hungr, O., Leroueil, S. and Picarelli, L., 2014. The Varnes Classification of Landslide Types, an Update. Landslides, vol. 11, p. 167–194.

Keefer, D.K., 1984. Landslides caused by earthquakes. Geological Society of America Bulletin, vol. 95, p. 406–421.

McKenna, K.M. and Lipovsky, P.S., 2014. Surficial geology, Dawson region, Yukon, parts of NTS 115O/14 & 15 and 116B/1, 2, 3, & 4. Yukon Geological Survey, Open File 2014-12, 1:25 000 scale.

Mortensen, J.K., 1988. Geology, southwestern Dawson map area, Yukon. Geological Survey of Canada, Open File 1927, 1:250 000 scale, https://doi.org/10.4095/130455.

Pánek, T. and Klimeš, J., 2016. Temporal behavior of deep-seated gravitational slope deformations: A review. Earth Science Reviews, vol. 156, p. 14–38, https://doi.org/10.1016/j.earscirev.2016.02.007.

Reuther, J., Potter, B., Coffman, S., Smith, H. and Bigelow, N., 2020. Revisiting the timing of the northern lobe of the White River Ash volcanic event in eastern Alaska and western Yukon. Radiocarbon, vol. 62, p. 169–188.

Tempelman-Kluit, D.J., 1980. Evolution of physiography and drainage in southern Yukon. Canadian Journal of Earth Sciences, vol. 17, p. 1189–1203, https://doi.org/10.1139/e80-125.